Participation of Endomembrane Cation/H$^+$ Exchanger AtCHX20 in Osmoregulation of Guard Cells[1][W][OA]

Senthilkumar Padmanaban, Salil Chanroj, June M. Kwak, Xiyan Li, John M. Ward, and Heven Sze*

Department of Cell Biology and Molecular Genetics, University of Maryland, College Park, Maryland 20742–5815 (S.P., S.C., J.M.K., X.L., H.S.); and Department Plant Biology, University of Minnesota, St. Paul, Minnesota 55108 (J.M.W.)

Guard cell movement is induced by environmental and hormonal signals that cause changes in turgor through changes in uptake or release of solutes and water. Several transporters mediating these fluxes at the plasma membrane have been characterized; however, less is known about transport at endomembranes. CHX20, a member of a poorly understood cation/H$^+$ exchanger gene family in Arabidopsis (*Arabidopsis thaliana*), is preferentially and highly expressed in guard cells as shown by promoter::β-glucuronidase activity and by whole-genome microarray. Interestingly, three independent homozygous mutants carrying T-DNA insertions in CHX20 showed 35% reduction in light-induced stomatal opening compared to wild-type plants. To test the biochemical function of CHX20, cDNA was expressed in a yeast (*Saccharomyces cerevisiae*) mutant that lacks Na$^+$(K$^+$)/H$^+$ antiporters (Δnhx1 Δnha1 Δkha1) and plasma membrane Na$^+$ pumps (Δena1-4). Curiously, CHX20 did not enhance tolerance of mutants to moderate Na$^+$ or high K$^+$ stress. Instead, it restored growth of the mutant on medium with low K$^+$ at slightly alkaline pH, but had no effect on growth at acidic pH. Green fluorescent protein-tagged CHX20 expressed in mesophyll protoplasts was localized mainly to membranes of the endosomal system. Furthermore, light-induced stomatal opening of the Arabidopsis mutants was insensitive to external pH and was impaired at high KCl. The results are consistent with the idea that, in exchanging K$^+$ for H$^+$, CHX20 maintains K$^+$ homeostasis and influences pH under certain conditions. Together, these results provide genetic and biochemical evidence that one CHX protein plays a critical role in osmoregulation through K$^+$ fluxes and possibly pH modulation of an active endomembrane system in guard cells.

One of the most fascinating processes in most land plants is the ability to regulate gas exchange and transpiration by the opening and closing of the stomatal aperture. The movement of a pair of special epidermal cells, the guard cells, controls the size of the stomatal aperture and so determines the extent of water loss via transpiration and of CO$_2$ uptake into the leaf for photosynthetic carbon fixation. At the beginning of the day, light stimulates the opening of the stomatal aperture of most plants by increasing solute concentration and decreasing water potential, thus attracting water into the guard cells (for review, see Assmann, 1993; Schroeder et al., 2001; Roelfsema and Hedrich, 2005). The increase in turgor pressure causes the guard cells to swell and pushes the pair of cells apart, increasing the aperture between the two cells.

At dusk, the aperture size decreases and becomes nearly closed at night, thus reducing transpiration and gas exchange. During drought, the amount of abscisic acid (ABA) reaching the guard cells can increase, triggering the efflux of ions and loss of water and turgor pressure, leading to closure of the stomatal aperture. ABA also prevents light-induced stomatal opening (Schroeder et al., 2001).

Although our knowledge of cellular signaling and osmoregulation in guard cells has advanced significantly in the last decade, the osmotic changes driving guard cell movement have focused mainly on the roles of plasma membrane (PM)-associated transporters and signaling elements regulating the transporters (Blatt, 2000; Fan et al., 2004; Roelfsema and Hedrich, 2005). Advances have been triggered by the ability to patch guard cell PM, to study transport across this membrane, and to analyze mutants. Light-induced stomatal opening starts when light activates the PM H$^+$-ATPase causing membrane hyperpolarization. K$^+$ then enters via inward-rectifying channels, and anions enter via predicted H$^+$/Cl$^-$ and H$^+$/NO$_3^-$ symporters. Ion, malate, and sugar accumulation decreases the water potential; thus, water is taken up, increasing turgor pressure. Several inward-rectifying K$^+$ channels (e.g. KAT1, KAT2, AKT1) in stomatal opening have been identified at the molecular level (for review, see Very and Sentenac, 2003; Fan et al., 2004). Nitrate is one counterion that balances K$^+$ uptake via an H$^+$-coupled NO$_3^-$ symporter (AtNRT1.1; Guo et al., 2003). Stomatal closing begins when the membrane depolarizes,

causing the opening of outward-rectifying K^+ channels. Dark-induced depolarization is caused by deactivation of the PM H^+ extrusion pump and by opening of anion efflux channels. Loss of K^+ and anions leads to a decrease in solute concentration, water efflux, and loss of guard cell turgor. GORK is suggested to be the major outward-rectifying K^+ channel (Hosy et al., 2003); however, the molecular identity of PM R-type and S-type anion channels is still unclear. Genetic evidence suggests that the AtMRP5 ABC (ATP-binding cassette) transporter mediates anion efflux (Klein et al., 2003).

Less well understood are the changes of intracellular compartments during guard cell movement. As guard cells increase in volume, the size of vacuoles increases considerably (Louget et al., 1990), indicating that the bulk of solutes entering guard cells accumulate in the large vacuoles (MacRobbie, 1999), which is iso-osmotic with the cytosol. When stomata close, guard cells are filled with numerous relatively small vacuoles. Many vacuolar transporters identified in plant cells are expressed in guard cells according to the Affymetrix 8K GeneChip results (Leonhardt et al., 2004). Endomembrane compartments, including vacuoles, are acidified by electrogenic H^+-pumping vacuolar-type ATPases (V-ATPase) and H^+-pumping pyrophosphotases (Sze, 1985; Rea and Poole, 1993). Thus, it is very likely that the vacuolar membrane potential ($\Delta\Psi_{vac}$) slightly positive inside the lumen relative to the cytosolic side and ΔpH acidic inside the lumen relative to the cytosol could drive the accumulation of K^+ into the lumen via H^+/cation antiporters. Anions, including Cl^- and NO_3^-, were predicted to enter vacuoles via anion-specific channels because these anions rapidly dissipate the membrane potential generated by the V-ATPase of intracellular vesicles (Sze, 1985), although recent evidence showed that NO_3^- enters vacuoles through a H^+-coupled NO_3^- antiporter (ClC-a) at the vacuolar membrane (De Angeli et al., 2006). VK channel activity previously characterized to function in K^+ release from vacuoles in response to elevated cytosolic Ca^{2+} (Ward and Schroeder, 1994) is mediated by TPK1/KCO1 (Bihler et al., 2005). FV channels are inhibited by elevated cytosolic Ca^{2+} and may modulate K^+ uptake into vacuoles during stomatal opening (Pei et al., 1999). It is unclear how most of these transporters are integrated with guard cell movement.

Here, we provide genetic evidence for the role of a novel endomembrane transporter in guard cell movement. Arabidopsis (*Arabidopsis thaliana*) CHX20 belongs to a large family of 28 cation/proton exchangers whose functions are largely unknown (Sze et al., 2004). Functional expression of CHX20 in a salt-sensitive yeast (*Saccharomyces cerevisiae*) strain suggests that it has a role in pH regulation and K^+ transport. Intriguingly, CHX20 is preferentially expressed in guard cells, and *chx20* null mutants showed a reduction in light-induced stomatal opening. Together, these results provide evidence that a member of the CHX family plays a critical role in osmoregulation of guard cells.

RESULTS

AtCHX20 cDNA Isolation and Predicted Protein

To obtain CHX20 (At3g53720) cDNA, total RNA was extracted from rosette leaves of 3-week-old Arabidopsis plants and first-strand cDNA was used to amplify the coding sequence. The primers at the start and end of the open reading frame (ORF; X20Cf and X20Cr; Supplemental Table S1) were designed based on the genomic sequence. A 2.5-kb fragment was amplified and its sequence (AY926476) matched the coding sequence that is formed from five exons (Fig. 1A).

The predicted CHX20 protein of 842 residues has two domains: (1) a hydrophobic domain (434 residues) with 10 to 12 transmembrane spans at the amino half; and (2) a large hydrophilic domain of 403 residues at the carboxylic end (Fig. 1B). The hydrophobic domain shows extensive similarity (56.5% similarity, 33.6% identity; E value of 1e-54) to the transmembrane domain of yeast ScKHA1 protein, although the long carboxylic tail of the two proteins did not align (10.6% identity; no E value; Supplemental Fig. S1). These results suggest that the transport activities of AtCHX20 and yeast ScKHA1 are similar.

Function of AtCHX20 in Yeast

To test the transport function of CHX20, the coding sequence was cloned in pYES-DEST52 yeast expression vector under the Gal promoter. Yeast mutants with disrupted *kha1* gene alone exhibited no obvious phenotype (Maresova and Sychrova, 2005), so we expressed CHX20 in a yeast mutant (KTA40-2). This strain lacks functional vacuolar and PM-localized Na^+/H^+ antiporters, PM Na^+ pumps ($\Delta nhx1$ $\Delta nha1$ and $\Delta ena1$-4), as well as the putative K^+/H^+ exchanger ($\Delta kha1$; Maresova and Sychrova, 2005). Strain KTA40-2 is highly sensitive to salt and to high K^+, so the transformant (KTA40-2-CHX20) was tested for its ability to grow on moderate levels of Na^+ and very high K^+. Surprisingly, mutant yeast expressing AtCHX20 was consistently more sensitive on media containing 100 mM Na^+ or 500 mM K^+ at various pH (Fig. 2A) than the mutant yeast harboring the vector alone. KTA40-2 mutants grew as well as CHX20 transformants on standard synthetic complete (SC) medium. These results suggest that CHX20 does not confer tolerance to salt stress.

Intriguingly, AtCHX20 enhanced KTA40-2 yeast mutant growth on slightly basic medium with no added K^+. At an external pH of 4.5 to 7.0, mutants grew relatively well with no added K^+. In fact, at acidic pH between 4.5 and 6.5, mutants grew consistently better than yeast transformants carrying CHX20. Curiously, growth of mutants carrying the vector alone was retarded at pH_{ext} 7.5, whereas transformants harboring CHX20 continued to grow as well as at pH 4.5 (Fig. 2B). Thus, strains carrying CHX20 had an advantage when the external pH was 7.5, suggesting that CHX20 conferred an ability to sustain growth at slightly basic pH.
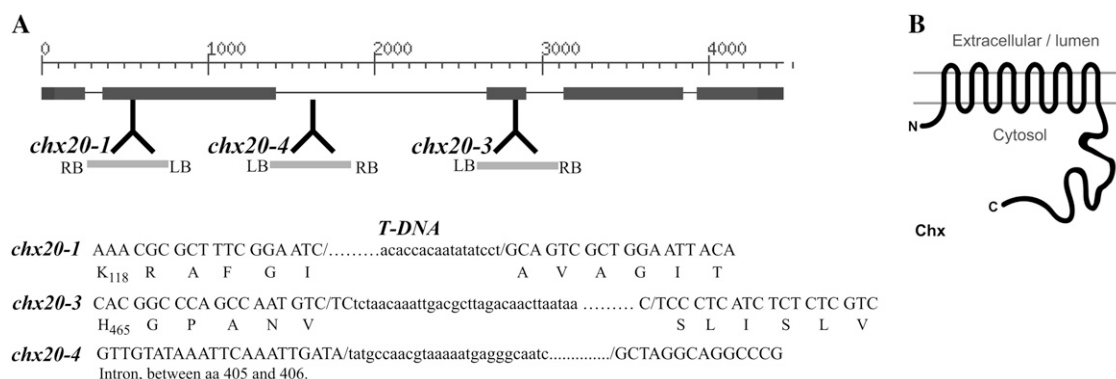
Figure 1. CHX20 gene organization and protein sequence. A, Genomic structure of CHX20 was confirmed by the cDNA (accession no. AY926476). The positions of three independent T-DNA insertional mutants are shown. The T-DNA sequences are shown in lowercase. Mutants chx20-1 and chx20-3 correspond to SALK lines SALK_031420 and SALK_011726, and chx20-4 was obtained from Genoplante. B, Predicted topology of AtCHX20 in the membrane (see Supplemental Fig. S1 for protein sequence).

We tested the effect of external K^+ concentration on yeast growth at pH 7.5. Transformants harboring CHX20 consistently grew better than KTA40-2 mutants as long as the K^+ level was kept low, from approximately 0.4 to 3 mM (Fig. 2C). When no exogenous K^+ was added, the agar medium contained about 0.4 mM K^+. Increasing external KCl concentration beyond 25 mM decreased the beneficial effect of CHX20. Because K^+ is required to sustain growth of all cells, the enhanced growth of transformants at low K^+ levels would suggest that CHX20 has a role in acquiring K^+ when the external pH is slightly alkaline or in maintaining suitable cellular homeostasis for growth. This idea is supported by nearly similar growth exhibited by yeast mutants carrying either vector alone or CHX20 when K^+ is raised to 50 mM.

Yeast KHA1 was shown before to confer tolerance to hygromycin (Maresova and Sychrova, 2005) as confirmed here in the AXT3 strain (Fig. 3A). This strain has a functional wild-type KHA1 but lacks three Na transporters (ena1-4Δ nha1Δ nhx1Δ). However, although transformants expressing CHX20 grew well at pH 5.5, they showed no growth in the presence of 150 μM hygromycin B. CHX20 did promote growth of mutants grown on yeast nitrogen base (YNB) medium at pH 7.5 similar to yeast KHA1 (Fig. 3B). These results suggest that CHX20 and KHA1 share similar, but not identical, activities.

AtCHX20 Is Preferentially Expressed in Guard Cells

Analyses of a guard cell transcriptome (Leonhardt et al., 2004; J. Kwak, N. Leonhardt, and J.I. Schroeder, unpublished data) revealed that only one member of the CHX gene family was highly expressed in guard cells. CHX20 showed little or no expression in mesophyll cells, whereas several other genes, such as CHX17, showed low to moderate expression (Fig. 4A). Furthermore, CHX20 expression is particularly strong in guard cells as shown by the 2-fold increase in normalized relative expression of CHX20 compared to that of

AtKAT1, a K^+ channel preferentially expressed in guard cells (Nakamura et al., 1995).

To verify the microarray results, CHX20 promoter-driven GUS activity was determined. Arabidopsis (Columbia [Col]) plants were transformed with a construct containing a 2-kb region upstream of the CHX20 ORF transcriptionally fused to the GUS reporter gene. T2 seeds were collected from six independent transgenic lines and all six lines of CHX20::GUS analyzed gave similar expression patterns. Striking GUS activity was observed in guard cells located in expanded cotyledons and in hypocotyls of 1-week-old seedlings (Fig. 4B, a). Three-week-old rosette leaves (Fig. 4B, d and e) and cauline leaves also showed very high GUS staining in guard cells. However, GUS staining was not detected in leaf pavement epidermal cells or in mesophyll cells. Interestingly, GUS activity was also detected in guard cells of floral organs, including the sepal, anther (Fig. 4B, b and c), and carpel (data not shown). GUS activity was not detected in the differentiated cells of roots, although CHX20 expression was only observed in the root cap of 1-week-old seedlings (Fig. 4B, f), consistent with the microarray results of root cap cells (P. Benfey, personal communication). Thus, analyses of both CHX20 promoter-GUS expression and guard cell-specific transcriptome data clearly indicate selective expression of CHX20 in guard cells.

AtCHX20-GFP Is Localized to Endomembranes

When transiently expressed in Arabidopsis mesophyll protoplasts, CHX20-GFP was visualized at the periphery of the nucleus and in the cytosol (Fig. 5A, f), suggesting that it is localized at the endoplasmic reticulum (ER) or in endomembranes. The CHX20-GFP signal was compared with those from a soluble GFP, GFP tagged to an ER retention sequence (GFP-HDEL), or to markers such as sialyltransferase (ST)-GFP for trans-Golgi, GFP-CPK9 for PM, and GFP-δTIP for vacuolar membrane (Fig. 5A). Although CHX20-GFP appeared to be localized to endomembranes, its
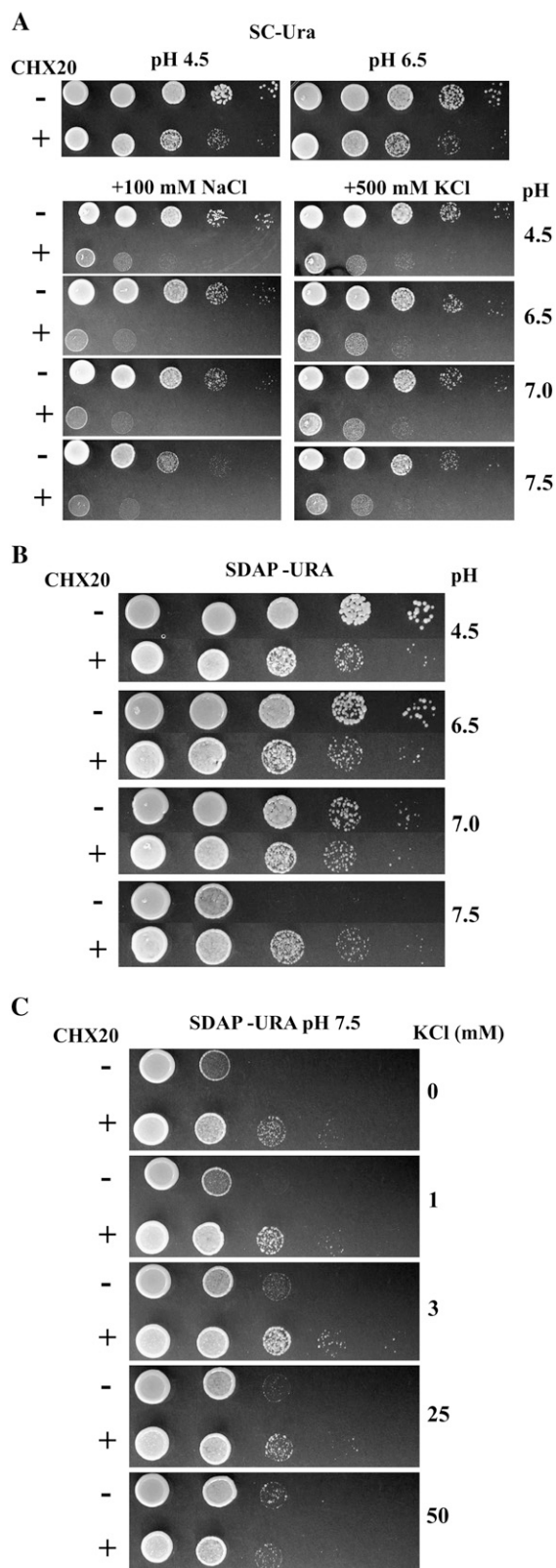
Figure 2. Yeast mutant KTA40-2 expressing CHX20 is tolerant to low K$^+$ at alkaline pH. A, Sensitivity to moderate NaCl stress and high KCl. CHX20 (+) or vector only (−) was expressed in a KTA40-2 mutant. Growth was tested on standard SC medium (containing 8 mM K$^+$, 1.7

pattern did not coincide entirely with any of the markers tested. To determine its location more precisely, the CHX20-GFP and a Golgi marker, ST-red fluorescent protein constructs, were cotransfected into mesophyll protoplasts. Of the cells that coexpressed both probes, the pattern of green fluorescence-labeled structures for the most part did not overlap with that of the red fluorescence (data not shown), indicating that CHX20 is not restricted to the trans-Golgi membrane.

Stably transformed plants expressing cauliflower mosaic virus 35S-driven CHX20-GFP also showed perinuclear fluorescent signals in guard cells (Fig. 5C), whereas soluble free GFP appeared inside the nucleus. Strong fluorescent signals were also detected inside the cytoplasm of cells expressing CHX20-GFP relative to that expressing the free GFP control. Together, the results suggest that CHX20 is localized to a subpopulation of endomembranes, although the protein does not appear to be a fixed resident of either the ER, Golgi, vacuole, or PM. We postulated that CHX20 is associated with vesicles/membranes that traffic among various subcellular membranes (Jurgens, 2004).

To test this idea, we examined the distribution of an endosome marker, Ara6-GFP (Ueda et al., 2001), and of CHX20 at several focal planes. Fluorescent signals of these two proteins were strikingly similar in several independent experiments. At the medial plane, the signal was cytoplasmic and at or near the PM (Fig. 5B). At the submedial focal plane, fluorescent signals were mostly cytoplasmic surrounding the plastids (Fig. 5B, data not shown). At the peripheral focal plane, the CHX20-GFP signal included several punctate regions. The GFP-tagged CHX20 was functionally active as shown by its ability to restore growth of KTA40-2 yeast at alkaline pH (Fig. 3B). Ara6, a Rab5-related GTPase, is distributed on a subset of endosomes and is involved in regulating vesicular transport (Ueda et al., 2001). These results suggest that an active CHX20 protein is associated with endosomal membranes.

Identification of *chx20* Null Mutants

To determine the in planta function of CHX20, we obtained three independent T-DNA insertional lines of Arabidopsis *chx20*. Two lines, *chx20-1* and *chx20-3*, were identified in the SIGnAL database (Alonso et al., 2003), and one line, *chx20-4*, was obtained from Genoplante (France). To confirm the T-DNA insertion site and select homozygous lines, PCR-based screening
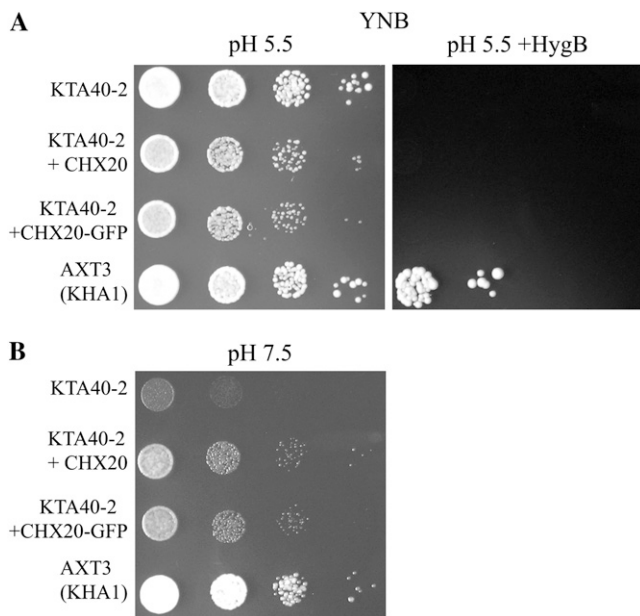
A

B

Figure 3. CHX20 fused to GFP is functionally active. KTA40-2 yeast (*ena1-4Δ nha1Δ nhx1Δ kha1Δ*) was transformed with empty pDR196 vector, CHX20, or CHX20-GFP. AXT3 (*ena1-4Δ nha1Δ nhx1Δ*) was transformed with empty vector and served as a native ScKHA1 positive control. Cells were serially diluted 10-fold and spotted on YNB plates. A, CHX20 did not confer tolerance to hygromycin. Five microliters of yeast was spotted on YNB medium at pH 5.5 with or without hygromycin B (150 μg/mL) and incubated for 4 d. B, CHX20 fused to GFP conferred tolerance to the KTA40-2 strain at basic pH. Yeast was spotted on medium adjusted to pH 7.5 with Arg base and incubated for 2 d.

was performed using CHX20-specific primers and T-DNA primers. Sequencing of the PCR-amplified fragments confirmed that a T-DNA insertion was located within exon 2 at coding sequence base 477 of the *chx20-1* mutant, inside the third exon at the 1,299 coding sequence of *chx20-3*, and within the second intron of *chx20-4* (Fig. 1A). We tested for CHX20 transcripts in leaves of all the mutants. Reverse transcription (RT)-PCR was performed using CHX20 gene-specific primers located at either side of the T-DNA insertion using template cDNA reverse transcribed from total leaf RNA. No products were amplified, indicating an absence of messages in all three alleles (Fig. 6B). The *chx20* mutants showed no obvious morphological or growth differences compared to wild-type plants under standard growth conditions (Fig. 6A). Overall, the size and shape of the guard cells were indistinguishable between mutants and wild-type plants.

Impaired Stomatal Opening in *chx20* Mutants

The highly specific expression of *CHX20* in guard cells (Fig. 4) suggested that CHX20 plays a role in guard cell signaling and/or development. Because we did not notice any developmental defects in the *chx20* knockout mutants, we tested whether the *chx20* null

mutants had any altered stomatal movement. We first compared light-induced stomatal opening in mutants and wild-type plants. Excised leaves of *chx20-1*, *chx20-3*, and *chx20-4* mutants were first exposed to white light for 3 h in a solution containing 5 mM KCl and 10 mM MES at pH 6.15. In all three mutants, the stomata failed to open as widely as wild-type plants. The ratio of light-induced stomatal opening per guard cell length in wild-type plants and in mutants ranged from 0.072 to 0.076 and 0.042 to 0.047, respectively. Thus, stomatal opening was reduced by approximately 35% in *chx20* mutants (Fig. 7A). We reduced the external KCl concentration in the opening solution to 0.1 and 1.0 mM. The aperture size was reduced slightly in wild-type and mutant leaves exposed to 0.1 mM K^+ (Fig. 7B), implying that guard cell movement is limited at low K^+ concentration. However, *chx20* mutants still showed approximately 35% reduction in light-induced stomatal opening regardless of the external K^+ concentration, indicating that the defect is not due to limited K^+ level alone.

Using isolated epidermis, we found that light-induced stomatal opening was maximal at pH 6.1 and 7. At basic pH 7.5 and 8.0, light-induced opening was decreased in wild-type plants (Fig. 7C) consistent with inactivation by basic pH of inward-rectifying K^+ channels and activation of outward-rectifying K^+ channels in *Vicia fava* guard cells (Ilan et al., 1994, 1996). However, mutants appeared to be insensitive to an acidic apoplastic pH that stimulated stomatal opening of wild-type guard cells. Thus, the reduced stomatal aperture of *chx20* mutants was particularly apparent at pH 6.1 and 7.0. At pH 7.5 and 8.0, mutants showed reduced stomatal aperture nearly similar to that of wild type. Thus, *chx20* mutants appeared to be unresponsive to pH regulation of guard cell movement.

To test whether stomatal closure was affected, isolated epidermis of wild-type and *chx20* mutant leaves were first exposed to white light for 3 h to induce stomatal opening and then incubated in 1 μM ABA to induce closure. The decrease in stomatal aperture was measured at 30-min intervals for 3 h. Although the aperture size of wild-type plants was larger than that of mutants before ABA addition, the percentage of closure of wild type was higher than that of mutants at all times (Fig. 8). These results indicate that *chx20* mutants were responsive to ABA; however, mutants were delayed in stomatal closure compared to wild-type plants (Fig. 8). Results would suggest that CHX20 might also participate in events leading to stomatal closure.

DISCUSSION

Here we have discovered a new transporter that participates in guard cell movement. Nearly nothing is known about the roles of cation/proton antiporter (CPA) genes in guard cells, although several members of the superfamily, including NHX1, are expressed there. The AtCHX family was uncovered recently as a
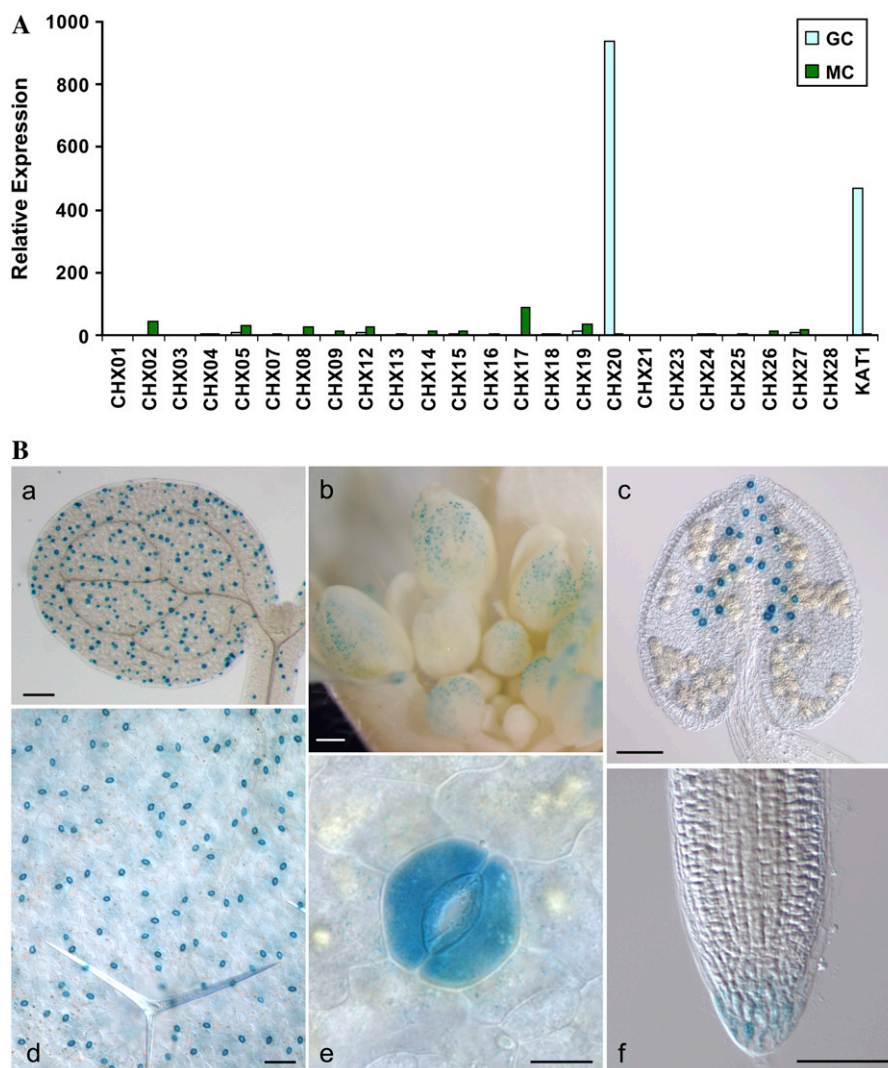
Figure 4. CHX20 is preferentially expressed in guard cells. A, Expression of the CHX gene family on the ATH1 whole-genome GeneChip. Microarray analysis was performed with RNA extracted from purified guard cells and from mesophyll cells of wild-type plants. Bar graph shows normalized expression levels of CHX genes present on the chip in guard cells (GC; light blue bars) and in mesophyll cells (MC; green bars). Relative expression of *KAT1*, a guard cell-expressed gene, serves as a positive control. B, CHX20 promoter activity. Promoter::GUS activity in cotyledon (a), sepals of young flowers (b), anther (c), rosette leaf (d), a magnified leaf (e), and root cap (f) is shown. GUS activity was seen after 2 h in 1.0 mM X-Gluc. Scale bars = 200 μm (a and b), 100 μm (c, d, and f), and 10 μm (e).

novel subfamily (Mäser et al., 2001; Sze et al., 2004), although the biochemical properties of this family remained uncharacterized until recently (Maresova and Sychrova, 2006). Previous studies showed 18 CHXs are preferentially expressed in pollen and six AtCHXs are highly expressed in roots and/or shoots (Cellier et al., 2004; Sze et al., 2004; Hall et al., 2006). However, a discrepancy in the spatial expression of CHX23 mainly in either pollen (Sze et al., 2004) or sporophytic tissues (Song et al., 2004) raises concerns about unconfirmed results. In this study, we find that CHX20 is preferentially expressed in guard cells using microarray and promoter::GUS analyses. Therefore, we tested the cellular function of AtCHX20 in yeast as a first step to understand its role in guard cell movement.

Role of AtCHX20 in K$^+$ Acquisition and pH Homeostasis in Yeast

Curiously, instead of conferring tolerance to moderate Na$^+$ stress or high K$^+$, CHX20 consistently caused

mutant KTA40-2 (Δena1-4 Δnha1 Δnhx1 Δkha1) to be more sensitive to salt. In another salt-sensitive yeast mutant, AXT3 (Δena1-4 Δnha1 Δnhx1), expression of AtCHX20 also resulted in increased sensitivity to moderate Na$^+$ stress and high K$^+$, although AtNHX1 or AtNHX2 conferred moderate tolerance to Na$^+$ stress (data not shown) as shown before (Yokoi et al., 2002). Furthermore, CHX20 was unable to confer hygromycin B tolerance. Thus, AtCHX20 is functionally distinct from the vacuolar AtNHX1 that sequesters excess Na$^+$ or K$^+$ into vacuoles and confers tolerance to high Na$^+$ or K$^+$ and to hygromycin B (Pardo et al., 2006).

Instead, CHX20 function appears to be important particularly when K$^+$ is depleted and when the external pH is slightly alkaline. This is shown by improved growth of KTA40-2 expressing CHX20 at pH 7.5 and when [K$^+$]$_{ext}$ was low (between 0.4 and 3 mM). Yeast growth and budding depends on the continuous uptake and accumulation of osmotic solutes, like K$^+$, especially when the external medium is depleted of this cation (Rodriguez-Navarro, 2000). The mechanism
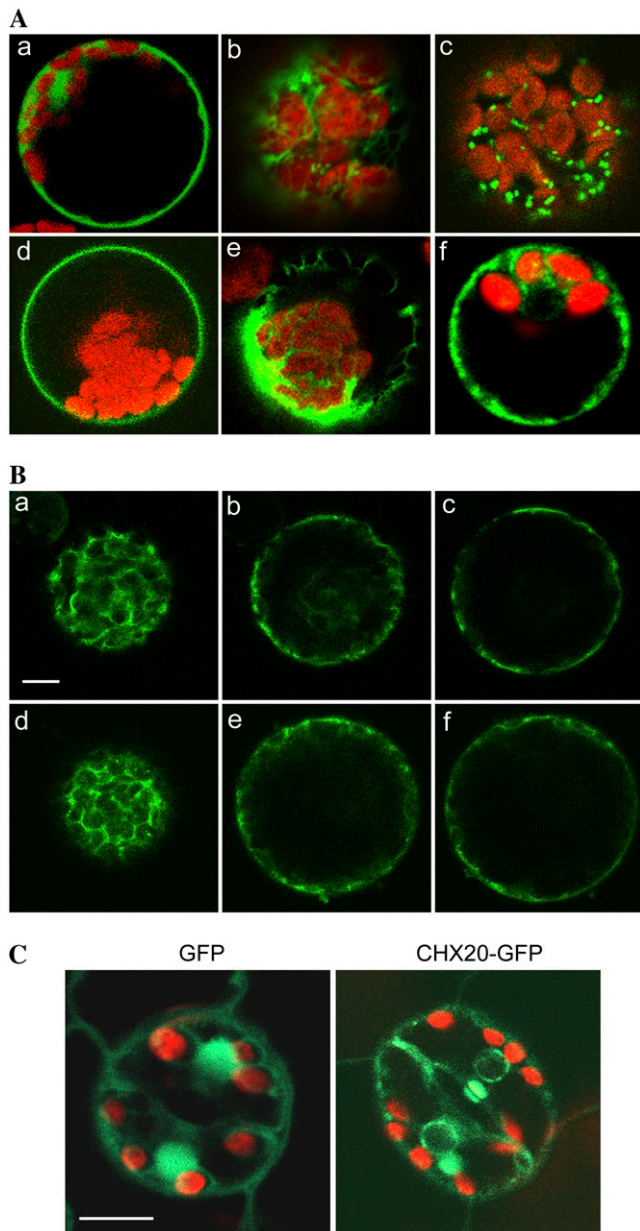
Figure 5. Endomembrane localization of CHX20-GFP protein. A, CHX20-GFP expression in Arabidopsis protoplast. Cauliflower mosaic virus 35S-driven GFP-tagged markers and AtCHX20-GFP (f) were transiently expressed in mesophyll protoplasts. Controls include free GFP (a); GFP tagged to HDEL (b); ST-GFP (c); Ca^{2+}-dependent protein kinase9 (GFP-CPK9; d); and vacuolar water channel (GFP-δ-TIP; e). Chloroplast autofluorescence is shown in red. B, Ara6-GFP and CHX20-GFP proteins show similar patterns of localization. CHX20-GFP (a–c) and Ara6 (d–f) are viewed at three optical planes from peripheral (a and d) to medial (c and f). Red emission is removed for clarity. Scale bar = 10 μm. C, CHX20-GFP in guard cells. Transgenic Arabidopsis plants expressing control 35S::pro-GFP (a) and 35S::CHX20-GFP (b) are shown. Cells or leaves were observed under a laser confocal microscope. Scale bar = 10 μm.

for K^+ uptake by CHX20 is not clear, although several observations are consistent with the idea that CHX20 participates in K^+ homeostasis through fluxes at intracellular compartments: (1) CHX20 is mainly localized to endomembranes, possibly endosomes, in plant cells; (2) phylogenetic analysis showed that CHX20 is a cation/proton antiporter belonging to the CPA2 subfamily (Sze et al., 2004); and (3) CHX20, like ScKHA1, enhanced yeast growth at basic pH when K^+_{ext} concentration was low (Maresova and Sychrova, 2005). Interestingly, KHA1 is also localized in yeast to endomembranes, possibly the Golgi. Because endomembrane compartments are acidified by V-ATPase in plants (Sze et al., 1999) as in yeast (Kane, 2006), cation accumulation into the lumen is most likely driven by the downhill influx of H^+ into the cytosol. Thus, one working model is that CHX20 is an endomembrane K^+/H^+ antiporter. In preliminary experiments, we did not detect an increase in K^+ content in yeast expressing CHX20, indicating that net changes in K^+ are small.

How are endomembrane compartments acidified when yeast is exposed to a basic medium? An important clue is provided by yeast *vma* (vacuolar membrane H^+-ATPase) mutants that cannot survive at pH 7.5, whereas wild-type yeast can. However, *vma* mutants grow at pH 5.5 (Nelson and Nelson, 1990), suggesting that mutants form acidic intracellular compartments through endocytosis of the extracellular medium (Munn and Riezman, 1994) and/or by passive uptake of acids (see Kane, 2006). The internalized compartment is apparently acidic enough to activate and energize the H^+-coupled transport of solutes needed to sustain *vma* mutant growth and to sort proteins in the secretory system. However, when the external medium is buffered at an alkaline pH, endocytosis would result in endosomal compartments with little or no pH gradient relative to the cytoplasm. Apparently, PMA1 (PM H^+-ATPase) alone is either inactivated or unable to generate a proton electrochemical gradient to support cell growth when the pH_{ext} is alkaline; thus, *vma* mutants succumb. However, wild-type yeast with functional VMA proteins sustains growth at pH 7.5, indicating that endomembrane compartments play a vital role in pH regulation and homeostasis. Our results indicate that, in addition to a vacuolar H^+-pump, CHX20 has a role in sustaining growth at pH 7.5 when other K^+ (Na^+)/H^+ antiporters are absent. Thus, CHX20 could fill a role in pH regulation.

What is the role of an endomembrane K^+/H^+ antiporter when external K^+ is low? We propose a model where CHX helps distribute cellular K^+ when the external pH is alkaline. It is well known that when medium K^+ is low or nearly depleted (<0.1 mM), energy-dependent K^+ uptake is needed to maintain $[K^+]_{cyt}$ at millimolar levels (Rodriguez-Navarro, 2000). However, when the medium pH is slightly alkaline, the proton-motive force for K^+/H^+ symport at the PM is reduced and the alkalinization of the cytosol could inactivate the PM H^+ pump. To counter the reduced
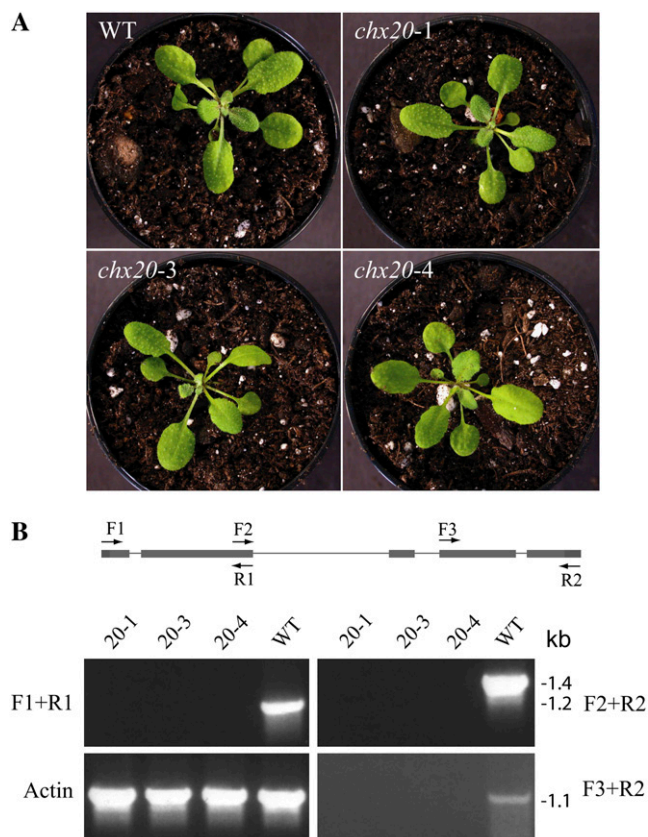
Figure 6. Three alleles of T-DNA insertional *chx20* mutants. A, Wild-type (WT) and mutant plants look similar. Sites of T-DNA insertion for *chx20-1*, *chx20-3*, and *chx20-4* mutants are shown in Figure 1A. B, Mutants lack CHX20 transcript. RNA isolated from leaves of *chx20-1*, *chx20-3*, and *chx20-4* and wild type was reverse transcribed. The cDNA product was PCR amplified with primers F1 and R1, F2 and R2, and F3 and R2 shown in the genomic structure (top). Actin11 is amplified as a loading control.

proton-motive force at the PM, acidification of intracellular compartments by yeast VMA could energize accumulation of K$^+$ from the cytosol into internal compartments using a K$^+$/H$^+$ antiporter. Due to the small volume of vesicles and internal compartments of the endomembrane system, a proton electrochemical gradient (acidic in the lumen) forms rapidly energizing K$^+$ accumulation. Accumulated K$^+$ can then be redistributed to the cytosol and other compartments by release via cation channels and by vesicle trafficking. Our results and model are consistent with genetic studies of a related protein, CHX17. K$^+$ starvation induced an increase of CHX17 transcripts in wild-type plants; and K$^+$ starvation caused a 20% decrease in K$^+$ content of *chx17* mutant roots (Cellier et al., 2004).

To offset alkalization of the cytosol in yeast grown at pH 7.5, we suggest that antiporters, like CHX20, neutralize cytosolic pH by mediating K$^+$ exchange for H$^+$ release from acidified compartments. The ability of CHX20-expressing KTA40-2 mutants to grow at pH 7.5 suggests that CHX20 is active at basic pH. Fungi and

plant V-ATPases show optimal activity in vitro at slightly alkaline pH (7.0–8.0) when PM H$^+$-ATPase is less active (Sze, 1985). Thus, two functions are proposed for CHX20: (1) H$^+$/K$^+$ antiport loads K$^+$ into intracellular compartments under conditions when mechanisms for active loading at the PM via H$^+$/K$^+$ symport are compromised; and (2) the cation/H$^+$ exchange maintains cytosolic pH homeostasis when cells are alkaline stressed.

The lack of a growth phenotype in yeast expressing CHX20 at pH 7.5 when K$^+_{ext}$ is replete suggests that other mechanisms take over to modulate K$^+$ and pH homeostasis when K$^+_{ext}$ is high (25–50 mM). Conceivably, high external K$^+$ could depolarize the cell membrane potential, increase K$^+$ influx into the cytosol and intracellular compartments, or both. With sufficient K$^+$ in the cell and intracellular compartments to support growth, the role of CHX20 may be shielded by other activities. Together, these results point to a role of CHX20 either in acquiring K$^+$ for cells under certain conditions or setting a suitable cellular pH homeostasis or both.

Model of AtCHX20 Function in Guard Cell Movement: Modulating Vesicle Trafficking

Our genetic studies demonstrate that CHX20 participates in guard cell movement, although its role in mediating stomatal opening may involve multiple tasks. Based on functional studies of yeast, it is reasonable to conclude that one role of CHX20 is to load guard cells with K$^+$. Stomatal aperture from *chx20* mutants failed to fully open after light induction. If CHX20 has a major role in K$^+$ loading, then the defect in opening might be minimized when K$^+_{ext}$ is not limiting. However, *chx20* mutants were impaired in stomatal opening whether the K$^+_{ext}$ was at 0.1 or 10 mM, when K$^+$ entry and content in cells in theory are not limited. These results suggest that CHX20 fills other roles. We tested whether CHX20 activity might be revealed at a different pH from that seen in KTA40-2 yeast. Stomatal opening was maximal at pH 6.0 to 7.0 and reduced at pH 7.5 to 8.0 in wild-type leaves, consistent with activation and deactivation by acidic pH of inward and outward K$^+$ channels, respectively, seen before (Ilan et al., 1994, 1996). Stomatal opening in mutants, however, failed to respond to acidic pH, suggesting that loss of CHX20 function could have interfered perhaps with pH homeostasis and with the activation and/or membrane trafficking of K$^+$ inward-rectifying channels.

Considering the large number of CPAs in plants (Mäser et al., 2001; Pardo et al., 2006), it is striking that single *chx20* mutants were impaired in stomatal opening. The contribution of other CHXs appears to be minimal in guard cells; however, cation/H$^+$ antiporters, like NHXs, are highly expressed in shoots, roots (Yokoi et al., 2002), and guard cells (Shi and Zhu, 2002; J.M. Ward, unpublished data). Members of this family (NHX1–NHX8) are localized to various membranes,
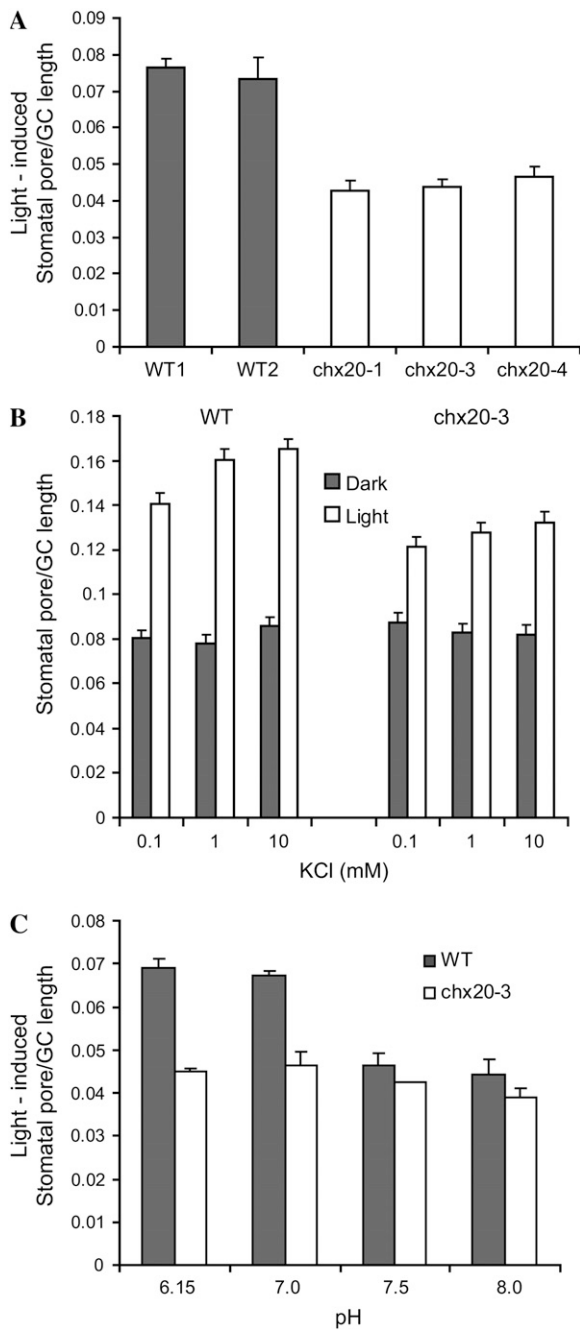
Figure 7. Light-induced stomatal aperture was reduced in *chx20* mutants. Aperture size is expressed as a ratio of maximal aperture size per length of guard cell (GC) pair. Twenty apertures were measured per treatment. Bar indicates SE. A, Three alleles show reduced stomatal opening. Excised leaves of dark-adapted wild type (WT1-2) and three mutants (*chx20*) were given 150 μE m^{-2} s^{-1} light or dark for 3 h. Leaves were placed in a solution containing 5 mM KCl and 10 mM MES-KOH at pH 6.15. Average light-enhanced pore size is shown from five independent experiments. B, Reduction in aperture size is independent of K$^+$ levels. Isolated epidermis from wild type and *chx20-3* were incubated separately in 10 mM MES-Tris at pH 6.15 without K$^+$ at dark for 3 h. KCl was then added to 0.1, 1, or 10 mM, and the epidermal strips were irradiated for 3 h as in A. Results of dark (gray) and light (white) treatment are from one representative experiment of three. C, Effect of pH on stomatal opening. Isolated epidermis from wild type

including the vacuole, prevacuolar compartment, Golgi, or PM (Venema et al., 2003; Pardo et al., 2006). If other endomembrane K$^+$ (Na$^+$)/H$^+$ antiporters are unable to substitute for CHX20 function, then CHX20 occupies a distinct functional niche. A simple model is that CHX20 function differs from other cation/H$^+$ exchangers because of (1) differential endomembrane localization; (2) different substrate affinity and specificity (K_m and V_{max}); and (3) differential modulation by pH and/or other signals and different interacting partners.

Confocal laser-scanning microscopy of guard cell vacuoles loaded with acridine orange revealed striking changes in the size and shape of vacuolar compartments during guard cell movement. Small vacuoles in cells surrounding closed stomata fuse with one another to form large vacuoles as stomata open (Gao et al., 2005). During closure, the large vacuoles break up into small vacuoles and undefined membrane structures. Moreover, pressure-induced guard cell swelling has demonstrated an increase in the PM area based on membrane capacitance measurements and increased K$^+$ conductance of both inward and outward rectifiers (Homann and Thiel, 2002; Meckel et al., 2005). These changes indicate incorporation of the exocytic vesicle with the PM. Guard cells undergo constitutive endocytosis and exocytosis even in turgid cells as shown by the uptake of impermeant fluorescent FM4-64 dyes into vesicles beneath the PM (Meckel et al., 2004). Although direct biophysical measurements are not yet available to measure vacuolar dynamics, electron microscopy (e.g. Louget et al., 1990) and live imaging support the idea that guard cells are active in vesicle/tubule budding from and fusion with vacuoles (Gao et al., 2005).

One model is that endomembrane-associated CHX20 exchanges K$^+$ for H$^+$ and accomplishes one or more purposes, including (1) bringing in external K$^+$ indirectly by accumulating K$^+$ in small intracellular compartments; (2) regulating pH in the cytosol as well as in the compartment lumen; and (3) perhaps participating in some way to facilitate membrane dynamics, including vesicle budding, trafficking, and fusion events required to bring about turgor and volume changes during guard cell movement (MacRobbie, 1999; Pratelli et al., 2004). The importance of pH for protein processing and sorting in the secretory and endocytic system is well recognized in yeast and animal cells (Paroutis et al., 2004), and this function is most likely conserved in plant cells (Sze et al., 1999). This idea is supported by a recent study showing that Arabidopsis H$^+$-pumping V-ATPase is required for endocytic and secretory trafficking (Dettmer et al., 2006).

and *chx20-3* were separately incubated 3 h in the dark in 5 mM KCl buffered to pH 6.15, 7.0, 7.5, or 8.0. Epidermal strips were exposed to light for 3 h. Average ratio of light-stimulated aperture/GC length of three independent experiments is shown.
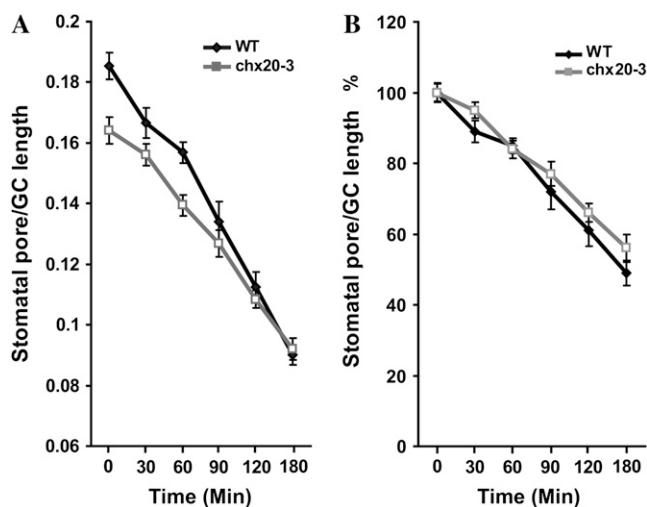
Figure 8. ABA-induced stomatal closure. Isolated epidermal cells from wild type or *chx20-3* were incubated in opening solution for 3 h under light. Then ABA was added to 1.0 μM and stomatal pore and guard cell length was measured at 30-min intervals. A, ABA reduces aperture size. Size is expressed as a ratio of maximal aperture size per length of guard cells. B, Percentage of closure. The relative percentage of closure is estimated using the light-induced aperture at zero time as 100%. Data are from two independent experiments. Bar = SE.

This study provides genetic evidence for a role of an endomembrane CHX in osmoregulation and in guard cell movement and working ideas to further test CHX cellular function. As the only AtCHX expressed in guard cells, CHX20 is an attractive model to understand the function and regulation of other CHX proteins (Sze et al., 2004). The transmembrane domains and the hydrophilic carboxylic tails of CHX members are highly conserved, suggesting a role in integrating signals with osmoregulation and possibly membrane trafficking. Significantly, this study highlights the active involvement of multiple transporters associated with intracellular membranes, including endosomal vesicles, in signaling, osmoregulation, and movement.

MATERIALS AND METHODS

Plant Materials and Growth Conditions

All experiments were conducted with Arabidopsis (*Arabidopsis thaliana*) ecotype Col-0. Wild-type, mutant, and transgenic plants were grown under the same conditions. Plants were grown in Miracle-Gro potting soil (Scotts). Seeds in soil were stratified at 4°C for 3 d and then plants were grown in controlled-environment chambers at 20°C under illumination of 150 μE m^{-2} s^{-1} with a 16-h photoperiod. Two weeks after germination, plants were given Miracle-Gro plant food at 20-d intervals. To test for promoter::GUS expression, transgenic seeds were grown under light (150 μE m^{-2} s^{-1}) at 20°C on plates containing 0.5× Murashige and Skoog (1962) salts and 1.0% agar, pH 5.8.

cDNA Cloning and DNA Constructs

Promoter::GUS

The AtCHX20 promoter was transcriptionally fused to the GUS gene. A 2-kb region upstream of CHX20 was amplified by PCR. Primers CHX20-PF

and CHX20-PR have *Sal*I and *Bam*HI restriction sites, respectively (see Supplemental Table S1 for all primers). The amplified products were digested and fused with GUS in pRITA I plasmid. Clones were confirmed by sequencing. The region containing the CHX20 promoter and GUS was subcloned into the binary vector pMLBart using *Not*I and named CHX20::GUS (Supplemental Table S2).

AtCHX20 cDNA

To isolate CHX20 cDNA, total RNA was isolated from leaves of wild-type Arabidopsis and first-strand cDNA was synthesized using reverse transcriptase. Primers X20Cf and X20Cr were used to amplify the cDNA by 25 cycles (94°C 30 s, 55°C 30 s, and 72°C 90 s). The forward and reverse primers contain *attB1* and *attB2* sequences (Supplemental Table S1) for Gateway recombination cloning. Gel-purified PCR products were recombined with pDONR221 using BP Clonase according to the manufacturer's method (Invitrogen). Resulting clones were sequenced using forward and reverse M13, S1, S2, and S3 primers. The correctly spliced clone with the longest ORF was named entry clone pECHX20.

To make a CHX20-GFP fusion construct, the CHX20 coding sequence from pECHX20 was recombined to the binary vector pK7FWG2 (Karimi et al., 2002) using LR Clonase to give an in-frame fusion of enhanced GFP at the C tail of CHX20 or pDCHX20-GFP. For expression in yeast (*Saccharomyces cerevisiae*), CHX20 from pECHX20 was recombined into a yeast-*Escherichia coli* shuttle vector, pYES-DEST52, to yield pDYES-CHX20.

Transformation of Plants

The binary vectors with CHX20 promoter::GUS or pDCHX20-GFP were introduced stably into Arabidopsis using *Agrobacterium tumefaciens*-mediated floral dip (Clough and Bent, 1998). Transformants were selected on 0.5× Murashige and Skoog plates containing kanamycin (50 μg mL^{-1}) or on soil by spraying with BASTA. T2 plants were analyzed for GUS expression or CHX20-GFP fluorescence. pDCHX20-GFP or other GFP-tagged constructs (see Supplemental Materials and Methods S1; Supplemental Table S2) were transiently expressed in onion (*Allium cepa*) epidermal cell or in Arabidopsis mesophyll protoplasts (Kovtun et al., 2000) and observed after 12 to 16 h.

Microscopy

GFP

The cells or tissues from transient and stable transformants were imaged for GFP fluorescence using a Zeiss LSM 510 laser-scanning confocal microscope with a 10× dry 0.8 numerical aperture lens and a 63× 1.2 numerical aperture water immersion lens (Zeiss). The filter settings are Ex 488 nm/Em BP 510 to 530 nm for GFP, and Ex 488 nm/Em LP 570 nm for chlorophyll. Sometimes optical sections of approximately 5-μm increments were made to visualize the signal patterns at the medial to the peripheral plane. Images were assembled in Photoshop (Adobe).

GUS Staining

At least six independent transgenic lines were tested for GUS activity. Tissues were incubated in a mixture containing 84 mM sodium phosphate, pH 7.0, 0.5 mM potassium ferrocyanide, 0.5 mM potassium ferricyanide, 0.5% Triton X-100, and 1.5 mM 5-bromo-4-chloro-3-indolyl-β-D-GlcUA (X-Gluc) at 37° C for 2 h. Samples were then fixed in 70% ethanol overnight to clear chlorophyll. Photographs were taken under a Nikon stereoscopic zoom microscope SMZ1000 or with differential interference contrast using a Nikon E600 microscope.

ATH1 GeneChip Analysis

The ATH1 23K GeneChip experiment was performed with guard cell and mesophyll cell RNA extracted from wild-type plants using methods described for the 8K chip (Leonhardt et al., 2004; see Supplemental Materials and Methods S1). Overall intensity normalization for the entire probe set was performed using Affymetrix Microarray Suite 5.0. Using the GeneChip Suite 5.0 default parameters, the detection P value and the signal value were

Padmanaban et al.

calculated for each probe set from each independent guard cell and mesophyll cell hybridization.

Yeast Strains and Growth Conditions

Yeast Strains

Yeast strains used in the study are (1) AXT3 (MATα his3-11 leu2-112 trp1-1 ade2-1 ura3-1 ena4Δ::his3::ena4Δ nha1Δ::leu2 nhx1Δ::trp1 in W303-1B); (2) KTA40-2 (MATα ade2-1 can1-100 his3-11,15 leu2-3,112 trp1-1 ura3-1 mal10 ena1Δ::his3::ena4Δ nha1Δ::lew2 nhx1Δ::trp1 kha1Δ::kanMX); and (3) LMB 01 (MATα ade2-1 can1-100 his3-11,15 leu2-3,112 trp1-1 ura3-1 mal10 ena1Δ::his3::ena4Δ nha1Δ::leu2 kha1Δ::kanMX) (Quintero et al., 2000; Maresova and Sychrova, 2005). Yeast was transformed with plasmid DNA using the lithium acetate method (Gietz et al., 1992) and the resulting transformants were selected on SC medium minus Ura (0.67% YNB, 2% Glc, 2% drop-out mix, 2% agar).

Determination of Growth

Fresh cells grown in liquid medium were washed and suspended in water and then adjusted to OD_{600} of 1.0 (1×). Ten-fold serial dilutions of the cells were prepared with sterile water and 5 μL of each dilution was spotted on plates containing appropriate SC minus Ura (0.67% YNB, 2% Glc or Gal, 2% drop-out mix minus Ura, 2% agar) or SDAP minus Ura and adjusted to the desired pH. To reduce K^+ and NH_4^+, modified SDAP medium was used. SDAP minus Ura medium consisted of 10 mM Arg-HCl (or Arg base), 2% (w/v) Glc or Gal, 2% drop-out mix minus Ura, 2 mM $MgSO_4$, 0.9 mM $CaCl_2$, trace minerals, vitamins, and 2% agar. Medium containing Arg-HCl was adjusted to pH 4.5 with tartaric acid and to pH 5.5 to 6.0 with 10 mM HEPES and Tris. For pH 7.0 to 7.5, medium contained Arg base and 10 mM HEPES and was adjusted to desired pH with tartaric acid or Tris. Plates were incubated at 30°C for 2 d and the relative growth of yeast was recorded using a Nikon Coolpix995 digital camera.

For some experiments, 3-d yeast cells were cultured in liquid YNB medium containing 0.67% YNB without amino acids, 2% Glc, 0.01% adenine, 0.01% Trp, and 10 mM MES adjusted to pH 5.5 with Arg base and grown for 18 h at 30°C. One-milliliter cultures were diluted to 6 mL with YNB medium without Glc and then starved for 18 h at 30°C. Starved cells were washed with 6 mL water, pelleted, and suspended in water. Cell density was normalized to OD_{600} of 0.2 and subjected to 10-fold serial dilution. Five-microliter aliquots were spotted on modified YNB plates at pH 7.5 or 5.5. The YNB medium also contained 2% agar, 0.02% bromocresol purple (catalog no. 860891; Sigma), and 20 mM MES adjusted to either pH 5.5 or 7.5 with Arg base. Hygromycin B, when added, was 150 μg/mL (catalog no. H7772; Sigma). Plates were incubated at 30°C for 2 to 4 d.

Arabidopsis T-DNA Mutant Analyses

T-DNA insertional mutants of chx20 (Alonso et al., 2003) were detected in the SALK database (http://signal.salk.edu/cgi-bin/tdnaexpress). Homozygous mutants, SALK_031420 (chx20-1), and SALK_011726 (chx20-3) seeds were first identified by PCR using LBa1 primer and CHX20-specific primers: CHX20-1-LP, CHX20-1-RP, CHX20-3-LP, CHX20-3-RP, CHX20-4F-P1, and CHX20-4F-P2 (Supplemental Table S1). The site of insertion was verified by sequencing.

To detect CHX20 transcript, total RNA isolated from chx20-1, chx20-3, and chx20-4 mutant and wild-type plants was reverse transcribed. Primer sets (Supplemental Table S1) F1 (from −15 to 30 bp) and R1 (1,300–1,252 bp); F2 (1,252–1,300 bp) and reverse primer R2 (3′-untranslated region); and F3 (1,506–1,541 bp) and R2 are expected to amplify products of 1,230, 1,413, and 1,158 bp in wild-type plants, respectively.

Guard Cell Movement

To test light-induced stomatal opening (Kwak et al., 2001), leaves were excised from 3-week-old wild-type and chx20 mutants. Leaves were separated into two batches and placed in aluminum foil-covered containers in the opening solution (5 mM KCl and 10 mM MES-KOH at pH 6.15) for 3 h. The dark-adapted leaves were then exposed to white light (approximately 150 μE

m^{-2} s^{-1}) or dark for 3 h at 20°C. Leaves were blended and filtered through 200-μm nylon mesh. Isolated epidermis was observed under a microscope (Axiovert, 40 CFL; Zeiss), and 20 stomata were measured for each condition. To study the effect of KCl concentration, isolated epidermal cells from wild type or chx20-3 were incubated in 10 mM MES-Tris at pH 6.15 without K^+ for 3 h in the dark and then KCl was added to a final concentration of 0.1, 1, and 10 mM before exposure to 3 h of light. To test pH, the pH 6.15 medium was buffered with 10 mM MES-Tris and that of pH 7.0 to 8.0 was adjusted with 10 mM HEPES-Tris. To test ABA-induced stomatal closure, isolated epidermal cells from wild type or chx20-3 were incubated in opening solution with light for 3 h, then ABA was added to 1 μM and stomatal pore size and guard cell length were measured at 30-min intervals using Scion image analysis. The stomatal aperture was measured as the maximal width between the inner cuticular lips.

Sequence data from this article can be found in the GenBank/EMBL data libraries under accession number AY926476 (AGI no. At3g53720).

Supplemental Data

The following materials are available in the online version of this article.

Supplemental Figure S1. AtCHX20 and ScKHA1 proteins.

Supplemental Table S1. Primer sequences.

Supplemental Table S2. Vectors used.

Supplemental Materials and Methods S1. Plant transformation and microarray analysis.

LITERATURE CITED

Alonso JM, Stepanova AN, Leisse TJ, Kim CJ, Chen HM, Shinn P, Stevenson DK, Zimmerman J, Barajas P, Cheuk R, et al (2003) Genome-wide insertional mutagenesis of Arabidopsis thaliana. Science **301:** 653–657

Assmann SM (1993) Signal transduction in guard cells. Annu Rev Cell Biol **9:** 345–375

Bihler H, Eing C, Hebeisen S, Roller A, Czempinski K, Bertl A (2005) TPK1 is a vacuolar ion channel different from the slow-vacuolar cation channel. Plant Physiol **139:** 417–424

Blatt MR (2000) Cellular signaling and volume control in stomatal movements in plants. Annu Rev Cell Dev Biol **16:** 221–241

Cellier F, Conéjéro G, Ricaud L, Luu DT, Lepetit M, Gosti F, Casse F (2004) Characterization of AtCHX17, a member of the cation/H^+ exchangers, CHX family, from Arabidopsis thaliana suggests a role in K^+ homeostasis. Plant J **39:** 834–846

Clough SJ, Bent AF (1998) Floral dip: a simplified method for Agrobacterium-mediated transformation of Arabidopsis thaliana. Plant J **16:** 735–743

De Angeli A, Monachello D, Ephritikhine G, Frachisse JM, Thomine S, Gambale F, Barbier-Brygoo H (2006) The nitrate/proton antiporter AtCLCa mediates nitrate accumulation in plant vacuoles. Nature **442:** 939–942

Dettmer J, Hong-Hermesdorf A, Stierhof YD, Schumacher K (2006) Vacuolar H^+-ATPase activity is required for endocytic and secretory trafficking in Arabidopsis. Plant Cell **18:** 715–730

Fan LM, Zhao Z, Assmann SM (2004) Guard cells: a dynamic signaling model. Curr Opin Plant Biol 7: 537–546

Gao XQ, Li CG, Wei PC, Zhang XY, Chen J, Wang XC (2005) The dynamic changes of tonoplasts in guard cells are important for stomatal movement in *Vicia faba*. Plant Physiol 139: 1207–1216

Gietz D, Jean AS, Woods RA, Schiestl RH (1992) Improved method for high efficiency transformation of intact yeast. Nucleic Acids Res 20: 1425

Guo FQ, Young J, Crawford NM (2003) The nitrate transporter AtNRT1.1 (CHL1) functions in stomatal opening and contributes to drought susceptibility in Arabidopsis. Plant Cell 15: 107–117

Hall D, Evans AR, Newbury HJ, Pritchard J (2006) Functional analysis of CHX21: a putative sodium transporter in Arabidopsis. J Exp Bot 57: 1201–1210

Homann U, Thiel G (2002) The number of K$^+$ channels in the plasma membrane of guard cell protoplasts changes in parallel with the surface area. Proc Natl Acad Sci USA 99: 10215–10220

Hosy E, Vavasseur A, Mouline K, Dreyer I, Gaymard F, Poree F, Boucherez J, Lebaudy A, Bouchez D, Very AA, et al (2003) The Arabidopsis outward K$^+$ channel GORK is involved in regulation of stomatal movements and plant transpiration. Proc Natl Acad Sci USA 100: 5549–5554

Ilan N, Schwartz A, Moran N (1994) External pH effects on the depolarization-activated K$^+$ channels in guard cell protoplasts of Vicia faba. J Gen Physiol 103: 807–831

Ilan N, Schwartz A, Moran N (1996) External protons enhance the activity of the hyperpolarization-activated K$^+$ channels in guard cell protoplasts of Vicia faba. J Membr Biol 154: 169–181

Jurgens G (2004) Membrane trafficking in plants. Annu Rev Cell Dev Biol 20: 481–504

Kane PM (2006) The where, when and how of organelle acidification by the yeast vacuolar H$^+$-ATPase. Microbiol Mol Biol Rev 70: 177–191

Karimi M, Inze D, Depicker A (2002) GATEWAY vectors for Agrobacterium-mediated plant transformation. Trends Plant Sci 7: 193–195

Klein M, Perfus-Barbeoch L, Frelet A, Gaedeke N, Reinhardt D, Mueller-Roeber B, Martinoia E, Forestier C (2003) The plant multidrug resistance ABC transporter AtMRP5 is involved in guard cell hormonal signaling and water use. Plant J 33: 119–129

Kovtun Y, Chiu W-L, Tena G, Sheen J (2000) Functional analysis of oxidative stress-activated MAPK cascade in plants. Proc Natl Acad Sci USA 97: 2940–2945

Kwak JM, Murata Y, Baizabal-Aguirre VM, Merrill J, Wang M, Kemper A, Hawke SD, Tallman G, Schroeder JI (2001) Dominant negative guard cell K$^+$ channel mutants reduce inward-rectifying K$^+$ currents and light-induced stomatal opening in Arabidopsis. Plant Physiol 127: 473–485

Leonhardt N, Kwak JM, Robert N, Waner D, Leonhardt G, Schroeder JI (2004) Microarray expression analyses of Arabidopsis guard cells and isolation of a recessive abscisic acid hypersensitive protein phosphatase 2C mutant. Plant Cell 16: 596–615

Louget P, Coudret A, Couot-Gastelier J, Lasceve G (1990) Structure and ultrastructure of stomata. Biochem Physiol Pflanz 186: 273–279

MacRobbie EAC (1999) Vesicle trafficking: a role in trans-tonoplast ion movements? J Exp Bot 50: 925–934

Maresova L, Sychrova H (2005) Physiological characterization of Saccharomyces cerevisiae kha1 deletion mutants. Mol Microbiol 55: 588–600

Maresova L, Sychrova H (2006) Arabidopsis thaliana CHX17 gene complements the kha1 deletion phenotypes in Saccharomyces cerevisiae. Yeast 16: 1167–1171

Mäser P, Thomine S, Schroeder JI, Ward JM, Hirschi K, Sze H, Talke IN, Antmann A, Maathius FL, Sanders D, et al (2001) Phylogenetic relationships within cation-transporter families of *Arabidopsis thaliana*. Plant Physiol 126: 1646–1667

Meckel T, Hurst AC, Thiel G, Homann U (2004) Endocytosis against high turgor: intact guard cells of Vicia faba constitutively endocytose fluorescently labeled plasma membrane and GFP-tagged K$^+$-channel KAT1. Plant J 39: 182–193

Meckel T, Hurst AC, Thiel G, Homann U (2005) Guard cells undergo constitutive and pressure-driven membrane turnover. Protoplasma 226: 23–29

Munn AL, Riezman H (1994) Endocytosis is required for the growth of vacuolar H$^+$-ATPase-defective yeast: identification of six new END genes. J Cell Biol 127: 373–386

Murashige T, Skoog F (1962) A revised medium for rapid growth and bioassays with tobacco tissue cultures. Physiol Plant 15: 473–497

Nakamura RL, McKendree WL Jr, Hirsch RE, Sedbrook JC, Gaber RF, Sussman MR (1995) Expression of an Arabidopsis potassium channel gene in guard cells. Plant Physiol 109: 371–374

Nelson H, Nelson N (1990) Disruption of genes encoding subunits of yeast vacuolar H$^+$-ATPase causes conditional lethality. Proc Natl Acad Sci USA 87: 3503–3507

Pardo JM, Cubero B, Leidi EO, Quintero FJ (2006) Alkali cation exchangers: roles in cellular homeostasis and stress tolerance. J Exp Bot 57: 1181–1199

Paroutis P, Touret N, Grinstein S (2004) The pH of the secretory pathway: measurement, determinants and regulation. Physiology (Bethesda) 19: 207–215

Pei ZM, Ward JM, Schroeder JI (1999) Magnesium sensitizes slow vacuolar channels to physiological cytosolic calcium and inhibits fast vacuolar channels in fava bean guard cell vacuoles. Plant Physiol 121: 977–986

Pratelli R, Sutter JU, Blatt MR (2004) A new catch in the SNARE. Trends Plant Sci 9: 187–195

Quintero FJ, Blatt MR, Pardo JM (2000) Functional conservation between yeast and plant endosomal Na$^+$/H$^+$ antiporters. FEBS Lett 471: 224–228

Rea PA, Poole RJ (1993) Vacuolar H$^+$-translocating pyrophosphatase. Annu Rev Plant Physiol Plant Mol Biol 44: 157–180

Rodriguez-Navarro A (2000) Potassium transport in fungi and plants. Biochim Biophys Acta 1469: 1–30

Roelfsema MR, Hedrich R (2005) In the light of stomatal opening: new insights into 'the Watergate'. New Phytol 167: 665–691

Schroeder JI, Allen GJ, Hugouvieux V, Kwak JM, Waner D (2001) Cell signal transduction. Annu Rev Plant Physiol Plant Mol Biol 52: 627–658

Shi H, Zhu JK (2002) Regulation of expression of the vacuolar Na$^+$/H$^+$ antiporter gene AtNHX1 by salt stress and abscisic acid. Plant Mol Biol 50: 543–550

Song CP, Guo Y, Qiu Q, Lambert G, Galbraith DW, Jagendorf A, Zhu JK (2004) A probable Na$^+$(K$^+$)/H$^+$ exchanger on the chloroplast envelope functions in pH homeostasis and chloroplast development in Arabidopsis thaliana. Proc Natl Acad Sci USA 101: 10211–10216

Sze H (1985) H$^+$-translocating ATPase: advances using membrane vesicles. Annu Rev Plant Physiol 36: 175–208

Sze H, Li X, Palmgren MG (1999) Energization of plant cell membrane H$^+$-pumping ATPase: regulation and biosynthesis. Plant Cell 11: 677–689

Sze H, Padmanaban S, Cellier F, Honys D, Cheng NH, Bock KW, Conejero G, Li X, Twell D, Ward J, et al (2004) Expression pattern of a novel gene family *At*CHX highlights their potential roles in osmotic adjustment and K$^+$ homeostasis in pollen biology. Plant Physiol 136: 2532–2547

Ueda T, Yamaguchi M, Uchimiya H, Nakano A (2001) Ara6, a plant-unique novel type Rab GTPase, functions in the endocytic pathway of *Arabidopsis thaliana*. EMBO J 20: 4730–4741

Venema K, Belver A, Marìn-Manzano MC, Rodrìguez-Rosales MP, Donaire JP (2003) A novel intracellular K$^+$/H$^+$ antiporter related to Na$^+$/H$^+$ antiporters is important for K$^+$ ion homeostasis in plants. J Biol Chem 278: 22453–22459

Very AA, Sentenac H (2003) Molecular mechanisms and regulation of K$^+$ transport in higher plants. Annu Rev Plant Biol 54: 575–603

Ward JM, Schroeder JI (1994) Calcium-activated K$^+$ channels and calcium-induced calcium release by slow vacuolar ion channels in guard cell vacuoles implicated in the control of stomatal closure. Plant Cell 6: 669–683

Yokoi S, Quintero FJ, Cubero B, Ruiz MT, Bressan RA, Hasegawa PM, Pardo JM (2002) Differential expression and function of Arabidopsis thaliana NHX Na$^+$/H$^+$ antiporters in the salt stress response. Plant J 30: 529–539